CERN / SPSLC 96-16
SPSLC / I208
14 March 1996

Antihydrogen Production and Spectroscopy

M. H. Holzscheiter[a1], G. Bendiscioli[b], A. Bertin[c], G. Bollen[d], M. Bruschi[c] M. Charlton[e], M. Corradini[f], D. De Pedis[g], M. Doser[d], J. Eades[d], X. Feng[h] T. Goldman[a], J. Hangst[h], R. Hayano[i], R. J. Hughes[a], D. Horváth[j], N. S. P. King[a] K. Kirseboom[h], H. Knudsen[h], V. Lagomarsino[k], R. Landua[d], G. Laricchia[e] R. A. Lewis[l], E. Lodi-Rizzini[f], G. Manuzio[k], U. Marconi[c], J. Merrison[h], S. P. Møeller[h] G. L. Morgan[a], M. M. Nieto[a], M. Piccinini[c], R. Poggiani[m], A. Rotondi[b], P. Salvini[b] N. Semprini-Cesari[c], G. A. Smith[l], C. M. Surko[n], G. Testera[k], G. Torelli[m] E. Uggerhøj[h], L. Venturelli[f], A. Vitale[c], E. Widmann[d], T. Yamazaki[i], Y. Yamazaki[i] A. Zoccoli[c], D. Zanello[g]

a. Los Alamos National Laboratory, Los Alamos, New Mexico 87545, U.S.A.
b. Pavia University & INFN , Pavia, Italy
c. Bologna University & INFN, Bologna, Italy
d. CERN, CH1211 Geneva, Switzerland
e. Dept. of Physics & Astronomy, University College London, London, WC1E6BT, UK
f. Brescia University & INFN , Brescia, Italy
g. Rome University "La Sapienza" & INFN , Rome, Italy
h. Inst. for Physics & Astronomy, University of Aarhus, DK-8000 Aarhus C, Denmark
i. University of Tokyo, Tokyo, Japan
j. Research Institute for Particle and Nuclear Physics, H-1525 Budapest, Hungary
k. INFN Genoa, Via Dodecaneso 33, 16146 Genoa, Italy
l. Pennsylvania State Univ., 303 Osmond Laboratory, University Park, PA 16802, U.S.A.
m. Universita di Pisa, Dipartimento di Fisica, I-56100 Pisa, Italy
n. University of California at San Diego, La Jolla, CA 92093-0319, U.S.A.

[1]Spokesperson, Email: pbar@cernvm.cern.ch

ABSTRACT

The study of CPT invariance with the highest achievable precision in all particle sectors is of fundamental importance for physics. Equally important is the question of the gravitational acceleration of antimatter.

In the last years, impressive progress has been achieved at the Low Energy Antiproton Ring (LEAR) at CERN in capturing antiprotons in specially designed Penning traps, in cooling them to energies of a few milli-electron volts, and in storing them for hours confined to a small volume in space. Positrons have been accumulated in large numbers in similar traps, and ultra-low energy positron or positronium beams have been generated. Finally, steady progress has been made in trapping and cooling of neutral atoms.

Thus the ingredients to form antihydrogen at rest are at hand. We propose to investigate the different methods to form antihydrogen at low energy, and to utilize the best of of these methods to capture 1000 or more antihydrogen atoms in a magnetostatic trap.

Once antihydrogen atoms have been captured and cooled, standard spectroscopic methods can be applied to interrogate their atomic structure with extremely high precision and compare it to its normal matter counterpart, the hydrogen atom. Especially the $1S - 2S$ transition, with a lifetime of the excited state of 125 msec, offers the possibility to directly compare matter and antimatter properties at a level of 1 part in 10^{18}, providing a direct test of CPT in the baryon sector at this precision.

Additionally, spectroscopic methods have been used to study the gravitational acceleration of atoms and, if applied to a comparison of hydrogen and antihydrogen, can provide direct experimental tests of the Weak Equivalence Principle for antimatter at a high precision

In the first phase of the experiment we will study the formation, capture and behaviour of antihydrogen atoms in such an environment by measuring the formation and disappearance rates of antihydrogen with an appropriate detector. In the second phase, we will investigate the atomic structure of antihydrogen using Doppler-free two-photon spectroscopic techniques.

1 Introduction

The main implications of CPT invariance that can be deduced from the CPT theorem developed by Lüders [1], Pauli [2], Bell [3], and Jost [4] are that a particle and its antiparticle have equal and opposite electrical charges, and the same inertial masses, lifetimes, and gyromagnetic moments. A few of these predictions have been tested at very high precision. An indirect test of the equality of the K^0 and $\overline{K^0}$ masses [5], compared to the mass of the K^0, has set the scale of precision to better than 10^{-18}. Direct tests such as the equality of the electron and positron gyromagnetic ratios [6] (2.1×10^{-12}) and the equality of the proton and antiproton cyclotron frequencies in the same magnetic field (10^{-9}) [7] have achieved impressive, but significantly lower, precision. However, the test of CPT in the neutral kaon system is based on an indirect and model dependent connection between the measured properties of the decay amplitudes and the kaon mass matrix, and would constrain a new CPT-violating interaction. Such a new interaction is only constrained to be less than 10 % of the strength of the CP-violating interaction [8]. Furthermore, it has been pointed out by Wald [9] that the proof of CPT invariance requires the assumption of flat spacetime, and is thereby in direct contradiction to the curved spacetime required by gravitation.

CPT symmetry of quantum-electrodynamics requires that the gross structure, fine structure, hyperfine structure, and Lambshifts in hydrogen and antihydrogen are identical. Spectroscopic measurements of photon transition frequencies in antihydrogen could, in principle, be performed with very high precision, and comparison with the analogous transitions in hydrogen would test CPT-invariance with commensurate precision. In particular, the 1/8 second lifetime of the metastable $2S$ level allows an ultimate precision of the $1S - 2S$ two-photon transition of 10^{-18}, if the center of the spectral line can be determined to one part in 10^3 and the line width can be reduced to the quantum limit [10]. For a more detailed discussion of these and related issues see also reference [11].

A number of attempts to unify gravity with the electro-weak and strong interactions call into question the general belief that the gravitational acceleration of particles and their antiparticles should be identical. However, no experimental tests have been performed [12]. Spectroscopic methods have been used to determine the gravitational acceleration of atoms with an accuracy of 10^{-8} [13] and offer the possibility for gravity measurements on antihydrogen at a level of of 10^{-6} or better.

To perform such high precision spectroscopic experiments antihydrogen atoms must be produced with extremely low kinetic energies and, due to the expected low number of atoms available, should be confined in a small volume in space.

Several proposals to efficiently form antihydrogen atoms at low energy have been discussed:

The first approach uses continuum to bound-state transitions driven by a laser to increase the rate for the radiative recombination processes between antiprotons and positrons [14]. The second method utilizes the strong temperature dependency of the recombination cross section when ultra-cold antiprotons are mixed with a high-density positron plasma in a Penning trap [15], and the third method consists of a charge-exchange reaction between antiprotons and positronium atoms [16].

The second method theoretically has the highest rate, leading to almost instantaneous conversion of the trapped antiprotons to neutral antihydrogen. The main problem identified with this reaction is the fact that antihydrogen is produced in highly excited Rydberg states and may not be stable against field ionization in the electric field gradients present in the experiment.

In the third approach antihydrogen is produced directly in the ground state or (if excited positronium atoms are used [17]) in low-lying excited states. Therefore, the system is not as susceptible to field ionization and is directly accessible to spectroscopic measurements. A test experiment, attempting to produce hydrogen atoms from protons and positronium atoms colliding in a crossed beam geometry has been performed by some of our collaborators [18], and constitutes the first successful experimental demonstration of the recombination of electrons and protons into hydrogen at low energy. Initial results are in agreement with theoretical predictions for the cross section of this reaction.

2 Production and trapping of antihydrogen

While many of the individual steps of the proposed experiment have been carried out in separate experiments it will remain a big challenge to the project to integrate all these different methods into one experiment. In the first phase of the work proposed here we intend to develop and refine the accumulation schemes for positrons and antiprotons, transfer both constituents into a common experimental set-up for recombination and detect the formed antihydrogen through its annihilation. We intend to study the different routes to antihydrogen production and compare them with each other taking into account specific requirements of future experiments. Additionally, we will superimpose magnetic gradients forming a prototype neutral trap and study the capture efficiency into such a trap.

2.1 Experimental overview

Using the method of experiment PS200, which will be described briefly in the next section, antiprotons can be captured in an electromagnetic field configuration known as a Penning trap, and can be cooled to sub-eV temperatures by electron cooling. We plan to use our existing catching trap set-up (with small modifications) to accumulate 10^7 antiprotons from the antiproton source. At the current capture efficiency of 0.2% and an anticipated intensity of antiproton pulses from the Antiproton Decelerator (AD) of 2×10^7 antiprotons per pulse, this will require 250 pulses or approximately 15 hours at an anticipated time period of $2-3$ minutes between pulses. Once a sufficient number of antiprotons has been accumulated, the entire bunch will be transferred to the antihydrogen experiment.

Large numbers of positrons have also been accumulated in similar field configurations. The first challenge will consist of combining these two experiments, bringing the antiprotons and positrons in close contact for a time sufficiently long to allow the recombination process to take place. If a free positron is to be combined with the

antiproton (method one or two), one may use nested Penning traps. The negative antiprotons and the positive positrons are stored in two different potential wells in close proximity of each other and are passed through each other at the time of recombination. Alternatively a combined radio-frequency (Paul) and Penning trap, which can confine particles of opposite electric charge, can be used. Both types of traps can be loaded efficiently by injecting an intense pulse from an external positron accumulator, which is then recaptured in the recombination trap. For the third method, bringing the positron to the antiproton in form of a neutral positronium atom, positron accumulation in an external positron accumulator may be used to enhance the intensity of the positron beam used for positronium generation in the trap.

Once antiprotons and positrons have been recombined the confinement by the electric forces ceases and antihydrogen atoms will escape, hit the nearest wall, and annihilate. To confine the produced antihydrogen atoms magnetic gradients interacting with the magnetic moment of the atoms can be used by superimposing a strong magnetic gradient field onto the constant field necessary for the Penning trap.

In constructing such a combination or superposition of different traps one must also allow for access of laser beams needed for cooling the antihydrogen atoms for long term confinement and for precision spectroscopic measurements, as well as provide space and access for particle detectors providing the diagnostic measurements during the different stages of the experiment. In Fig. 1 we show a sketch of the entire lay-out depicting all components discussed in this short description.

2.2 Capture and cooling of antiprotons

2.2.1 The PS200 catching trap system

We have developed a method based on a combination of energy loss in material and electrodynamical capture of charged particles in a Penning trap (a superposition of a strong homogeneous magnetic field and an electric quadrupole field). Particles of 5.9 MeV kinetic energy are passed through a thin target foil and, with a proper choice of target thickness, up to 1.5% of the antiprotons emerge from the down-stream side of the target at energies below 30 keV [19]. These "low-energy antiprotons" are dynamically captured in a large volume "catching" Penning trap of 50 cm total length and 3.8 cm diameter, situated in the horizontal, cryogenic bore of a superconducting magnet capable of producing a magnetic field of up to 6 Tesla.

The trap structure consists of 7 electrodes: the entrance foil, a central region comprised of five cylinders (2 endcaps, 2 compensation electrodes, and the central ring) with lengths and diameters carefully chosen to produce a harmonic, orthogonalized, quadrupole potential in the central region [20], and a cylindrical high voltage exit electrode. For the purpose of the initial antiproton capture the trapping region is defined by the entrance foil and the high voltage exit electrode. This main section of the trap has no harmonic properties and will be referred to as the "catching trap" throughout this document. The central, harmonic region serves a dual purpose: to initially hold cold electrons in preparation for the electron cooling, and then to collect the cooled antiprotons after the electron cooling has taken place.

Figure 2 shows the general layout of the experimental set-up and the different detectors used to monitor the incoming beam and to verify the capture of antiprotons. A particle pulse from the accelerator is transported to the front end of the experiment, which contains a parallel plate avalanche counter (PPAC) for beam monitoring. Magnetic focussing in the 3.2 T field places a focal point at the final degrading foil. In this 135 micron gold coated aluminum foil at the trap entrance the antiprotons lose energy by collisions with the atoms of the foil material and, assuming proper adjustment of the additional degrader material upstream, an optimum number of low energy particles will exit from the downstream face of the foil. They will be reflected by the electrical potential at the far end of the trap and travel back towards the entrance electrode. A pulse derived from annihilations in the support structure of the PPAC windows is used to trigger the high voltage switch to ramp the entrance electrode up to full potential before the particles can escape, thereby capturing them within the volume of the trap.

2.2.2 Electron cooling of antiprotons in the trap

Once captured, the antiprotons may be cooled further by electron cooling. For this purpose a dense electron cloud is preloaded into the central, harmonic region of the catching trap. These electrons will cool by synchrotron radiation in the high magnetic field in a few minutes and will assume a thermal equilibrium at the ambient temperature of the trap. Typical electron clouds achievable in our trap contain about 10^9 electrons.

Kilo-electronvolt energy antiprotons will oscillate back and forth in the 0.5 meter long catching trap and interact with the electrons via Coulomb collisions, transfering their kinetic energy slowly to the cloud of electrons, which in turn transfers this energy to the external helium bath through synchrotron radiation. By this process the antiprotons will lose their kinetic energy and eventually settle also into the harmonic well at the center of the trap. During recent tests of this system we have succeeded in the capture of more than one million antiprotons from a single bunch from LEAR. Up to 65 % of the captured particles were cooled to sub-eV energies and collected in a 1 cm^3 region at the center of the trap.

An energy spectrum of these low energy antiprotons is shown in figure 3. The observed mean energy is below 1 eV with a FWHM of 800 meV. Both these values are upper limits only, since the Coulomb interaction between the charged particles is dominating these measurements. We therefore interpret these results as a demonstration that antiprotons have been cooled to thermal equilibrium with the temperature of the surrounding trap structure and the residual gas (typically at 10 K in these tests) within a few hundred seconds after initial capture.

2.3 Low energy positron accumulation

Controlled sources of low energy positrons, and their efficient conversion to Ps atoms at surfaces, have been reported for many years (for reviews see e.g. [21, 22]). Positrons emitted from radioactive sources have a range of energies in the MeV region and upon

penetrating solid matter slow typically within a few picoseconds to an energy close to the thermal level. Once the positron has slowed it is free to diffuse in the medium where most annihilate, with the diffusion length being typically 10^3 to 10^4 Å and dependent upon the moderator material. During the diffusion process a positron may encounter the surface of the solid and be spontaneously emitted into the surrounding vacuum as a free positron, or bound to an electron as positronium. Comparing the penetration depth with the diffusion length immediately sets the scale for moderator efficiencies of around 10^{-3} slow positrons per fast positron.

Once the positrons have been liberated into vacuum they can easily be manipulated and typical applications use beams with kinetic energies in the eV to tens of keV range [22, 23]. Such low energy positrons, if incident upon surfaces, can be re-emitted as positrons or as positronium atoms under controlled conditions. Now the efficiencies can be high, even approaching 100 % for positronium emission from some heated surfaces [22], since the implantation depths can be less than the diffusion length.

In order to facilitate the observation of antihydrogen it will be advantageous to have a pulsed positron/positronium source. We therefore intend to accumulate the continuous beam produced by a radioactive-source-based instrument and interfacing it to the recombination trap. The method proposed here derives from the work of Surko and collaborators [24, 25] who use a buffer gas (N_2 at low pressure) to moderate the slow positrons at a rate of around 5.5×10^4 $s^{-1}mCi^{-1}$. Thus from a 70 mCi (26 GBq) ^{22}Na source around 10^8 positrons can be accumulated in a period of three minutes and can be stored for about 30 minutes. Using a more efficient differential pumping scheme, adding a fourth (ultra-high vacuum) stage, and improving source and moderator geometry will enable us to accumulate 10^{10} positrons in much less than one hour. This set-up is illustrated schematically in figure 4. Successive stacks [25] of positrons can be introduced into the storage stage since the positron lifetime at a pressure of 10^{-11} Torr, is larger than 50 days. The stored positrons can then be released through valve A into the UHV recombination trap, where they can be either captured and stored again or allowed to form positronium by striking a suitably arranged surface.

Alternative methods of producing and accumulating low-energy positrons are being discussed in our collaboration at this time and include the production of short, intense pulses of positrons using a pulsed electron accelerator [26] and injecting these pulses directly into an UHV trap similar to the fourth stage mentioned above.

2.4 Antihydrogen formation

2.4.1 Historical background

A variety of schemes to produce antihydrogen have been proposed in the literature [27]. Amongst these, only the reactions listed below (with the appropriate references for detailed discussions) will yield the ultra-low energy antihydrogen atoms needed for precision spectroscopy and gravity studies with a rate sufficient for realistic ex-

perimentation:

$$e^+ + \bar{p} + h\nu \Rightarrow \overline{H} \tag{1}$$

(see Ref. [14]),

$$e^+ + e^+ + \bar{p} \Rightarrow \overline{H} + e^+ \tag{2}$$

(see Ref. [15]), and the two reactions

$$Ps + \bar{p} \Rightarrow \overline{H} + e^- \ , \tag{3}$$

$$Ps^* + \bar{p} \Rightarrow \overline{H^*} + e^- \ . \tag{4}$$

(See References [16], [17], [28], and [29], respectively.)

The antihydrogen atoms are typically produced in excited states with the principal quantum number of the intermediate state given by the dynamics of the specific process. In reaction (1) this state can be selected by tuning the laser stimulating the capture, in reaction (2) energy and momentum conservation lead to very highly excited states ($n \cong 100$), and in the last two reactions [(3) and (4)], mostly low-lying excited states are populated and can be partially selected by using positronium atoms in a specific excited state. In the first two cases, both constituents forming antihydrogen need to be trapped. In the last two cases, only antiprotons need to be confined before the recombination process since the positron is delivered in form of a positronium beam. Each method has distinct advantages and disadvantages and, depending on the final application, any one route could be the best choice. We therefore intend to pursue the routes via reaction 1,3, and 4 to find the method best suited to our final goal. However, if reaction 2 proves to be efficient, it could also be used.

2.4.2 Laser assisted recombination in a combined trap

The first proposal to form antihydrogen was presented by Budker [30] and was based on the spontaneous radiative recombination

$$e^+ + \bar{p} \Rightarrow \overline{H} + h\nu \ . \tag{5}$$

The rate for this reaction is small since the emission of a photon, necessary to conserve energy and momentum, is a slow process on the time scale of a collision. Therefore laser stimulated recombination (see reaction (2) and reference [14]) was proposed in which the rate would be increased by about two orders of magnitude for capture in particular $n-$states by illuminating the reaction region with photons of appropriate energy $h\nu$ corresponding to the particular continuum-bound state transition. For the hydrogen case, the predicted large enhancement factors have recently been observed on merged electron and proton beams in storage rings [31] - [33]. To take advantage of the enhancement by laser stimulation it is necessary to have positrons and antiprotons spend enough time near each other for the interaction to take place. Positrons and antiprotons have the opposite sign electrical charge and can not be trapped simultaneously in a Penning trap. To trap positrons and antiprotons (or electrons and protons) simultaneously in the same region of space a combined

Penning and RF-trap (Paul trap) may be used. Such a trap employs a homogeneous static magnetic field and a static electric quadrupole field for ion confinement (Penning trap). For electrons, the repelling force from the electrostatic field is overcome by a radio-frequency-quadrupole field (Paul trap), and positrons and antiprotons can be kept in the same volume for an indefinitely long time. This arrangement was first discussed by Schüssler et al. [34] for the capture of ions in flight. Further theoretical and experimental investigations of such a system were performed by Bate et al. [35]. The possibility to use such a system for the formation of antihydrogen was first mentioned by Guo-Zhong Li and G. Werth [36] who analysed the regions of stability for particles with vastly different charge-to-mass ratios (e^- and $^{238}U^{92+}$). Such a trap has recently been demonstrated [37] to hold several thousand electrons and protons simultaneously at estimated densities of 10^7 cm^{-3}, which is about 1/100 of the space charge limit. Plans to continue this experiment by attempting laser stimulated recombination of electrons and protons into hydrogen exist, and will be carried out in the near future.

2.4.3 Antihydrogen formation using a dense positron plasma

In the second process (see reaction (2)), the high positron density provides a second positron in the vicinity of a collision between antiprotons and positrons to assist in the conservation of energy and momentum. The rate constant for this process is strongly dependent on the relative velocity of positrons and antiprotons and varies with temperature as $T^{-9/2}$.

While the theoretical production rate for this process appears, at first sight, to be extremely high (with a 10^7/cm^3 positrons at 4.2 K one would convert 10^6 antiprotons stored in the trap into antihydrogen atoms within a time intervall of less than 200 milliseconds), two critical problems have been identified: Firstly, the antihydrogen atoms are created in an extremely high Rydberg state ($n = 100$ or larger). This gives rise to the possibility that these loosely bound systems are field ionized by the electric field gradients present in the trap. To address this question, the PS196 collaboration is planning to conduct a test experiment at the end of this LEAR running period. Secondly, the neutral atom traps available for antihydrogen only stabilize specific spin states (low-field seeking states), and a spin change during de-excitation from these high n levels to the ground state must be carefully avoided.

2.4.4 Antihydrogen by antiproton-positronium collisions

An alternative way to enhance the radiative antihydrogen formation rate by several orders of magnitude by coupling the recombination process to a third particle (for energy and momentum conservation) was first pointed out by B. Deutch and uses collisions between positronium atoms and antiprotons [16] (See reactions (3) and (4)). This process can be interpreted as Auger capture of the positron to the antiproton. Cross sections have been estimated by Humbertson, et al. [38], using charge conjugation and time reversal to link the well known cross section for positronium formation in collisions between positrons and hydrogen to the antihydrogen formation

cross sections. Early calculations assumed both the produced antihydrogen as well as the incoming positronium atom to be in the ground state, resulting in a production cross section of 3.2×10^{-16} cm^2 with a broad maximum at a $\overline{p}$ energy of 2.5 keV. Calculations of the total antihydrogen formation cross section occupying all possible quantum states of the antihydrogen using classical and semi-classical methods [39] have obtained values which are considerably larger than the ground-state results. Values for the formation of antihydrogen in specific excited states are given by Ermolaev, et al. [40] and exhibit a large cross section to low-lying excited states.

2.4.5 Recombination experiments with protons

To test the validity of the calculated cross-sections and to better identify experimental problems with the specific method of recombination, one can use the charge conjugate reaction, forming hydrogen by recombining electrons and positrons.

Such test experiments may be more difficult than the actual production of antihydrogen because of the difficulties of detecting hydrogen atoms amidst the natural background of hydrogen. Not only is it hard to distinguish the produced hydrogen atoms from those present in the residual gas, detection of low energy hydrogen atoms in general is much more difficult than the detection of antihydrogen atoms which have a very clear signature through their annihilation on normal matter.

To test the reactions (3) and (4), part of our collaboration has set up an experiment to perform the charge-conjugate experiment of forming hydrogen atoms via collisions between protons and positronium [41]. While designed specifically for testing the theoretical predictions for antihydrogen formation, this experiment also allowed us to develop the necessary technology of positronium production.

An event rate of $(8.1 \pm 3.1) \times 10^{-4}$ s^{-1} was obtained at a proton beam energy of 13.3 keV. This is in good agreement with expectations from available theory [42, 43] when the appropriate transformation for the velocity of the protons is taken into account. Data acquisition is continuing to improve the statistical accuracy and to make systematic background analyses.

2.5 Magnetic traps for antihydrogen

Having discussed the generation and trapping of all necessary components to form antihydrogen, the next task is to combine all this into an environment suitable for trapping and studying the neutral antihydrogen atoms. Much of the development work in this area will be guided by the excellent work by the groups at MIT [44, 45, 46], and Amsterdam [47], who have developed the technology to magnetically confine dense clouds of hydrogen atoms.

The confining force being the magnetic gradient, interaction with the magnetic moment of the atoms separates the (anti-)hydrogen into low field seeking atoms and high field seeking atoms. Even though work with hydrogen has been performed with both states, only the low field seeking states are of use in the case of antihydrogen, where collisions with the walls of the containment vessel are unacceptable. The trap configuration used for the latter case normally consists of an arrangement of coils,

designed to produce a magnetic minimum at the center of the trap without having a zero field location, which would introduce spin-depolarizing Majorana transitions. The essentially cylindrical geometry of these traps has been proposed by Pritchard et al. [44] and provides transverse trapping forces by a set of superconducting race track coils which generate a quadrupole field. Axial confinement is achieved through coaxial solenoids at either end of the trapping volume, which provide a barrier against axial leakage and also the non-zero field value in the center.

In filling the magnetic traps in the hydrogen work, the "gas" is allowed to fall into the potential well by inelastic collisions with residual gas atoms, a method unacceptable for antihydrogen. An alternative method we propose consists of superimposing the magnetic trap and the Penning trap in such a way that the Penning trap is located within the potential well for the confinement of the neutral atoms. Antihydrogen produced in the high-field seeking states would quickly leave the trap volume, while the low-field seeking states would be attracted towards the center. To achieve continuous confinement, the well depth will have to be substantially larger than the kinetic energy at which the antihydrogen is formed, or effective laser cooling needs to be employed, to quickly cool down the antihydrogen atoms after formation. Using 1.5 Tesla for the magnetic well depth, initial confinement would be limited to atoms with $T \leq 1$ Kelvin.

2.6 Antihydrogen detection

Detection of annihilating antihydrogen, and discrimination against antiproton annihilations in background gas and confining vessel, is of prime importance, both for the understanding of the process of recombination, as well as a diagnostic tool during all steps of the production and study of antihydrogen. The goals for this detector are:

- discrimination between antihydrogen, antiproton and positron annihilation
- reconstruction of the annihilation vertex with good resolution
- high rate capabilities to study the evolution in time of the $\bar{p}$ and e^+ clouds

The apparatus is shown in Fig. 1. The volume outside of the trap and in-between the racetrack coils houses five multiwire proportional chamber (PWC's) for charged tracking and vertex determination, followed by a CsI electromagnetic calorimeter (for detection of the two 511 keV γ's). The detectors have cylindrical symmetry, but are divided into quadrants for modularity, access and simple reconfiguration.

2.6.1 Charged track reconstruction

The charged tracking detector consists of 5 concentric multiwire proportional chambers (MWPC's) with anode layers situated at radii 5, 6, 7, 8 and 9 cm, and with an active length of 20 cm. Readout of the anodes (anode wire spacing of 2 mm) and of the cathode strips will provide a sufficient resolution in r-ϕ and z to reconstruct the $\bar{p}$ annihilation vertex to within about 1 mm.

The 2196 anode wires and cathode strips are read out via a PCOS III system.

The average thickness of one chamber can be as low as 0.5 x 10^{-3} radiation lengths, which gives a very small contribution to multiple scattering.

2.6.2 γ detection

The CsI calorimeter is a 20 cm long cylinder which lies at a radial distance of 10 cm, and consists of 1200 crystals with dimensions 1x1x6 cm^3. This granularity allows the position determination of two interacting 511 keV γ's - and thus of the production (annihilation) point - to approximately 1 cm. The overall detection efficiency for two 511 keV γ`s is about 50 %. In 6 cm CsI, minimum ionizing particles deposit 33.6 MeV, easily separable from 511 keV $\gamma$`s.

The presence of a strong, inhomogeneous magnetic field requires the use of photodiodes for the readout of the scintillation light. In addition, the CsI emission spectrum is most prominent at longer wavelengths, and thus better matched to the response of photodiodes than to photomultipliers. Due to the requirement of detecting photons down to 500 keV, noise is the dominant problem, and essentially limits the read-out options to avalanche photodiodes or state-of-the-art solid state photodiodes, which have the added advantage of a fast signal, allowing to reduce background via a tight time coincidence window. The shaping time is determined on the low side by the 0.9 μsec scintillation decay time of the crystals, and on the high side by pulse pile up considerations, and will thus be typically 3 μsec. For triggering purposes, we plan to use ADC's with fast conversion time (like LRS FERA's), and relatively low resolution (8 bits), covering the range 0 - 50 MeV.

The total assembly consists of four quadrants of 11 kg each.

3 Spectroscopy of antihydrogen

3.1 Possible experiments with antihydrogen

Considering the effort necessary to produce antihydrogen one must naturally ask the question what the physics benefits of such an endeavor would be. In principle, these can be found in two areas:

CPT tests by comparing spectroscopic measurements of hydrogen and antihydrogen.

Study of the antimatter gravity in the Earth's gravitational field.

The first would constitute a test of CPT at a level rivaling even the result on the kaon system, and especially would do so in the baryon sector, while the second experimental area would test the validity of the Weak Equivalence Principle (WEP) and possibly shed light on the problem of unifying gravity with the three other forces.

Over the last decade, the precision of spectroscopic studies of hydrogen has advanced enormously. Today the highest precision has been achieved for the hyperfine structure (6.4×10^{-13}) and for the $1S - 2S$ transition (1.8×10^{-11}). Based on the lifetime of the 2s state (1/8 second) and the natural linewidth connected to this, a possible precision of 10^{-18} has been discussed for the latter case [48]. This precision

would require using trapped hydrogen atoms, an environment which would be directly applicable to antihydrogen.

3.1.1 CPT tests with Antihydrogen

Currently the best tests of CPT invariance have been performed in the kaon system followed by precision comparisons of the magnetic moments and masses of the electron, positron, proton, and antiproton. The comparison of the inertial masses of the proton and the antiproton have now reached a precision of 1.1×10^{-9} [7].

The principles of high precision hydrogen spectroscopy are equally valid for antihydrogen (taking into account specific restrictions imposed on the handling of antihydrogen). As a specific example we would like to discuss the $1S - 2S$ transition, which promises the highest possible precision due to its long lifetime. More details on other transitions can be found in reference [11]. The energy interval of 2468 THz between the $n = 1$ and the $n = 2$ states of (anti)hydrogen is determined mainly by the (anti)Rydberg constant. The reduced mass correction contributes at the 0.5% level and contains information about the mass ratio of positron and antiproton. The $1S$ Lamb shift, which includes radiative corrections and vacuum polarization effects, contributes at the ppm-level. At the level of 1 part in 10^9 the influence of the finite nuclear charge radius appears.

One important practical difference between hydrogen and antihydrogen spectroscopy is the number of available atoms. This presents the challenge to develop methods which combine extreme detection sensitivity with the highest possible resolution. We generally assume that a cold sample of at least 10^3 antihydrogen atoms has been produced by recombination of antiprotons and positrons or positronium at 4 K. Since magnetic fields of the order of several Tesla will be necessary to trap both the constituents as well as the neutral atoms, Zeeman and Doppler broadening will be the dominant systematic effects. At the highest resolution, transit time broadening and the second order Doppler effect may also contribute.

Two-photon excitation methods are intrinsically Doppler-free and can be used to drive transitions between magnetic sublevels of equal Zeeman shifts, allowing us to neglect magnetic field inhomogeneities. However, the excitation rates are very low and this method is restricted to either trapped antihydrogen atoms (allowing long interaction times) or very high laser intensities ($> 5000\text{W/cm}^2$).

The extremely small natural linewidth of 1 Hz of the $1S - 2S$ transition makes this the ideal candidate for precision spectroscopy on hydrogen and antihydrogen. Doppler-free excitation is possible by the absorption of two photons from opposite directions. The relativistic Zeeman shift due to the magnetic field in this case is only 18 Hz/Gauss (for transition between the $m_F = +/- 1$ states). The ultimate resolution will then be mainly dependent on the temperature in the trap and is 300 kHz/K, i.e 900 Hz at 3mK.

In a dense atomic beam (10^9 atoms/cm^3) this transition has been observed with an accuracy of parts in 10^{12} [49] and the $1S-2S$ transition frequency has been measured with a precision of 1.8×10^{-11} by comparing the frequency of the excitation light at 1234 THz with that of a methane stabilized helium-neon laser at 88.5 THz [50].

3.1.2 Gravity studies using antihydrogen

An equally important question to be addressed is the one of possible differences of the gravitational acceleration of matter and antimatter (constituting a violation of the Weak Equivalence Principle). Gravity measurements on both (charged) antiprotons and (neutral) antihydrogen atoms have been discussed for many years, and our collaboration intends to address this question vigorously. Simple ballistic measurements of "g" on antihydrogen are difficult and unlikely to yield high precision measurement because of the photon recoil limit of approximately 2.4 mK. Consequently, a more elaborate method, using a horizontal beam of ultra-low energy antihydrogen atoms and interferometric techniques has been suggested [52]. If the formed antihydrogen atoms could be trapped and laser cooled more powerful methods may become available. One can look for the gravitational sag of the cold atoms in the shallow well of the (weak) magnetic traps. [51].

Or, if it is possible to form an atomic fountain, an even more powerful method could be developed based on the work of by Chu and collaborators [13]. In their experiment they used velocity-sensitive, stimulated Raman transitions to measure the gravitational acceleration, "g", of laser-cooled sodium atoms in an atomic fountain geometry. In the absence of external forces acting on the atoms the final state of an atom will depend on the phase of the driving Raman field. In the frame of reference falling with the atom, the Raman light fields appear linearly Doppler-shifted in time, which shows up as a phase shift varying as the square of the time. Distinct interference fringes were observed with an uncertainty in the phase determination of 3×10^{-3} cycles. This represented a sensitivity to "g" of $\delta g/g = 3 \times 10^{-8}$.

The much higher photon recoil limit for laser cooling hydrogen atoms (≈ 2.4 mK) gives an rms velocity spread of approximately 700 cm/sec. A much faster fountain beam, resulting in greatly increased experimental dimensions, will have to be used. Much less than 1 % of the initial population can be expected to contribute to the fringes. Nevertheless, this method is the only one identifiable in the current literature which shows the potential of a high precision measurement of "g" on antihydrogen atoms.

3.2 Other experiments with ultra-cold antiprotons

While the main thrust of our collaboration will go towards production, identification, trapping, cooling, and the study of antihydrogen at rest, a number of possibilities exist to employ the technology of antiproton trapping and cooling for small scale experiments in atomic and nuclear physics. The continuation of the work on trapping antiprotons in dense helium targets will continue and is the topic of a separate letter-of-intent. The need for lower energy antiprotons has led the PS205 collaboration to consider using a trap similar to the PS200 catching trap as a source for their experiment and an active discussion on these issues has been initiated. Additionally, a number of small scale experiments both in nuclear physics as well as in atomic physics are possible in a parasitic operation at the antiproton catching trap of our antihydrogen production set-up, and a number of members from our group have expressed

interest in continuing a line of research which has been part of the program of PS200 for the last two years, using a low energy extracted antiproton beam for collisional studies. Details of these experiments will be the topic of separate communications with the SPSLC.

4 Summary

Recent progress in trapping and storing low-energy antiprotons has created exciting opportunities for fundamental research in the areas of CPT violation and gravity. We propose to explore the most promising routes to produce antihydrogen. The goal is to generate antihydrogen atoms with low enough kinetic energy so that they can be captured into a magnetic gradient trap where they may be cooled further by laser radiation. With proper care of the vacuum environment the storage time of these atoms can reach times infinitely long on the scale of the intrinsic life times, therefore allowing spectroscopy at the limit of the natural linewidth. In this proposal we have discussed specifically the measurement of the $1S-2S$ transition, but similar methods can be used to study the hyperfine interaction or measure the Rydberg constant.

The availability of low energy antihydrogen atoms will also provide opportunities to study the gravitational acceleration of antimatter and matter in the Earth's gravitational field.

Appendix I: Experimental plans and milestones

The physics accessible with low energy antihydrogen is very diverse and based on the initial success we anticipate a long and healthy physics program including CPT and gravity tests. At the current time we concentrate mostly on the steps leading to the first spectroscopy of antihydrogen atoms. Studies on positron trapping and positronium formation will be performed independently from access to antiproton beams, as will be the development of the necessary laser technology for cooling and spectroscopy. It must be noted that all methods for trapping, cooling, and spectroscopy can be developed with hydrogen atoms, as long we keep in mind to use methods appropriate for antihydrogen as well. As soon as the new antiproton source will come on line, recombination experiments will commence, aiming towards trapping antihydrogen atoms in low lying excited states for spectroscopy.

Phase I:

1997 Reconfigure Antiproton Accumulator.
- (a) Development of the positron accumulator.
- (b) Upgrade of the PS200 catching trap.
- (c) Design of the magnetic trap.

1998 Installation and testing of key elements at the AD site.
- (a) Transfer of the PS200 catching trap to new source.
- (b) Installation and tests of the positron accumulator.
- (c) Installation and commisioning of the magnetic trap.

1999 Commisioning of the antiproton catching trap at the AD
- (a) First capture and cooling of antiprotons from the new source.
- (b) Stacking of antiprotons, establishing a sufficient density in the trap.
- (c) Accumulation and transfer of positrons at the AD site.

2000 Trapping of antihydrogen.
- (a) First formation and detection of low energy antihydrogen.
- (b) Establish reaction rates and test detection schemes.
- (c) Establish temperatures and final phase space for atom trapping.

2001 (a) Collection of antihydrogen in magnetic gradient trap.
- (b) Determine trapping efficiency of neutral atom trap.

Phase II:

2001+ Start of spectroscopy of antihydrogen.
- (a) Study laser cooling of antihydrogen in magnetic trap.
- (b) Spectroscopy of antihydrogen ($1s - 2s$ transition).
- (c) Gravitational studies

References

[1] G. Lüders; Det. Kon. Dan. Vid. Sel. Mat.-fys. Medd. 28 (1954) 1.

[2] W. Pauli, in: *Niels Bohr and the development of physics*, ed. W. Pauli, Pergamon, New York (1955) 30.

[3] J. S. Bell; Proc. Roy. Soc. A231 (1955) 479.

[4] R. Jost; *The general theory of quantized fields*; American Mathematical Society, Providence, Rhode Island (1965).

[5] R. Carosi et al.; Phys. Lett B 237 (1990) 303.

[6] R. S. Van Dyck, P. B. Schwinberg, H. G. Dehmelt; Phys. Rev. Lett. 59 (1987) 26.

[7] G. Gabrielse, D. Phillips, W. Quint, H. Kalinowsky, G. Rouleau; Phys. Rev. Lett. 74 (1995) 3544

[8] M. Kobayashi, A. I. Sanda; *On testing the CPT symmetry*, RU 92/3/8, Rockefeller University (1992).

[9] R. M. Wald; Phys. Rev. D 21 (1980) 2742.

[10] D. H. MacIntyre, T. W. Hänsch; Metrologia 25 (1988) 61

[11] M. Charlton, J. Eades, D. Horvath, R. J. Hughes, and C. Zimmermann; Physics Report 241 (1994) 65

[12] M. M. Nieto and T. Goldman, Phys. Rep. 205 (1991) 221; 216 (1992) 343.

[13] M. Kasevich and S. Chu, Appl. Phys. B54 (1992) 321.

[14] R. Neumann, H. Poth, A. Winnacker, and A. Wolf Z. Physik A313 (1983) 253

[15] G. Gabrielse, S. L. Rolston, L. Haarsma, and W. Kells, Phys. Lett. A 129 (1988) 38.

[16] B. I. Deutch et al., Phys. Scripta T22 (1988) 288.

[17] B. I. Deutch, M. Charlton, M. H. Holzscheiter, P. Hvelplund, L. V. Jørgensen, H. Knudsen, G. Laricchia, J. P. Merrison, and M. R. Poulsen; Hyperfine Interactions 76 (1993) 153

[18] J. Merrison, accepted for publication in Hyperfine Interactions

[19] M. H. Holzscheiter; Physica Scripta 46 (1992) 272

[20] G. Gabrielse, L. Haarsma, and S. L. Rolston; Int. J. Mass Spec. and Ion Processes 88 (1989) 319

[21] P.J. Schultz and K. G. Lynn; Rev. Mod Phys., 60 (1988) 701

[22] M. Charlton and G. Laricchia, Hyperfine Interactions 76 (1993) 97

[23] M. Charlton and G. Laricchia; J. Phys. B23 (1990) 1045

[24] T. J. Murphy, C. M. Surko; Phys. Rev. A46 (1992) 5696.

[25] R. G. Greaves, M. D. Tinkle, C. M. Surko; Phys. Plasmas 1 (1994) 1439

[26] M. Begemann, G. Gräff, H. Herminghaus, H. Kalinowsky, R. Ley; Nucl. Instr. Meth. 201 (1982) 287, and R. H. Howell, R. A. Alverez, M. Staneck; Appl. Phys. Lett. 40 (1982) 751

[27] M. H. Holzscheiter, Hyperfine Interactions 81 (1993) 71.

[28] B. I. Deutch, L. H. Andersen, P. Hvelplund, F. M. Jacobsen, H. Knudsen, M. H. Holzscheiter, M. Charlton, and G. Laricchia, Hyperfine Interactions 44 (1988) 271.

[29] M. Charlton, Phys. Lett. A 143 (1990) 143.

[30] G. I. Budker, A. N. Skrinskii; Sov. Phys. Uspekhi 21 (1978) 277

[31] U. Schramm et al., Phys. Rev. Lett. 67 (1991) 22

[32] F. B. Yousif et al.; Phys. Rev. Lett 67 (1991) 26

[33] A. Wolf, Hyperfine Interactions 76 (1993) 189

[34] Chun-Sing O, Hans A. Schüssler; J. Appl. Phys. 52 (1981) 2601.

[35] D. J. Bate, K. Dholakia, R. C. Thompson, D. C. Wilson; J. of Mod. Optics 39 (1992) 305.

[36] Guo-Zhong Li, G. Werth; Physica Scripta 46 (1992) 587

[37] J. Walz, S. B. Ross, C. Zimmermann, L. Ricci, M. Prevedelli, and T. W. Hänsch; to be published in Hyperfine Interactions (1996)

[38] J. W. Humberston, M. Charlton, F. M. Jacobsen, and B. I. Deutch, J. Phys. B20 (1987) L25.

[39] A. M. Ermolaev, B. H. Brandsen, and C. R. Mandel, Phys. Lett. A 25 (1987) 44.

[40] A. M. Ermolaev, Hyperfine Interactions 44 (1988) 375.

[41] M. Charlton, G. Laricchia, B. I. Deutch, X. Feng, J. S. Hängst, P. Hvelplund, H. Knudsen, J. P. Merrison, E. Uggerhoj, M. H. Holzscheiter, R. J. Hughes, and M. R. Poulsen, in: *Third Biennial Conference on Low Energy Antiproton Physics, LEAP'94* eds. G. Kernel, P. Krizan, M. Mikuz (World Scientific, Singapore) 1995 pp. 589-597.

[42] J. Mitroy, A. T. Stelbovics; J. Phys. B27 (1994) L79

[43] A. Igarashi, N. Toshima, and T. Shirai; J. Phys. B27 (1994) L497

[44] D. E. Pritchard; Phys. Rev. Lett. 51, 1336 (1983).

[45] H. F. Hess, G. P. Kochanski, J. M. Doyle, N. Masuhara, D. Kleppner, and T. Greytak; Phys. Rev. Lett. 59, 672 (1987).

[46] D. Kleppner, in The Hydrogen Atom, editors: G. F. Bassani, M. Inguscio, T. W. Hänsch; Springer Verlag, Berlin (1989) p. 103

[47] J. T. M. Walraven, R. van Roijen, and T. W. Hijmans; in *The Hydrogen Atom*; eds. G. F. Bassani, M. Inguscio, and T. W. Hänsch; Springer Verlag Berlin, Heidelberg (1989); and
J. T. M. Walraven; Hyperfine Interactions 76 (1993) 205.

[48] T. W. Hänsch,C. Zimmermann; Hyperfine Interactions 76 (1993) 47.

[49] M. Weitz, F. Schmidt-Kaler, T. W. Hänsch; Phys. Rev. Lett 68 (1992) 1120

[50] F. Schmidt-Kaler, D. Leibfried, S. Seel, C. Zimmermann, W. König, M. Weitz, T. W. Hänsch; Phys. Rev. A51 (1995) 2789

[51] W. Paul, Rev. Mod.Phys.62 (1990)531

[52] T. J. Phillips, in: *Third Biennial Conference on Low Energy Antiproton Physics, LEAP'94* eds. G. Kernel, P. Krizan, M. Mikuz (World Scientific, Singapore) 1995 pp. 569-578

Figure Captions

Fig. 1: Conceptual view of antihydrogen experiment at the Antiproton Decelerator at CERN.

Fig. 2: Schematic lay-out of antiproton catching trap of experiment PS200. Shown are the superconductive magnet dewar, the trap, and beam monitors and scintillators for antiproton detection.

Fig. 3: Energy spectrum of cooled antiprotons. The apparent mean energy is ≤ 1 eV and the apparent FWHM is ≤ 800 meV (see text also for details).

Fig. 4: Schematic illustration of a positron accumulator with ultra-high vacuum storage stage to interface to the PS200 antiproton trap. In the actual apparatus the trapping stage has three stages [24, 25].

Antihydrogen Production and Storage

Experimental Scheme

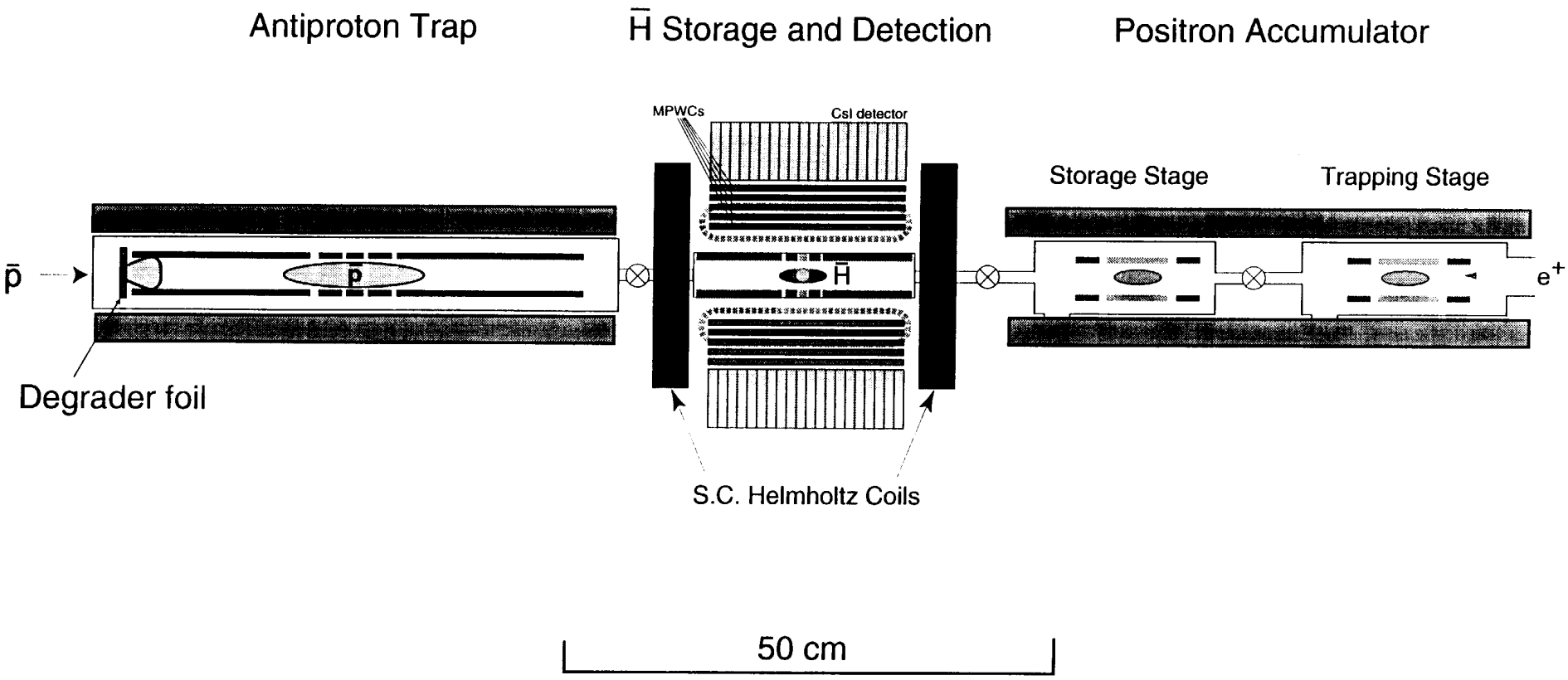

Fig. 1

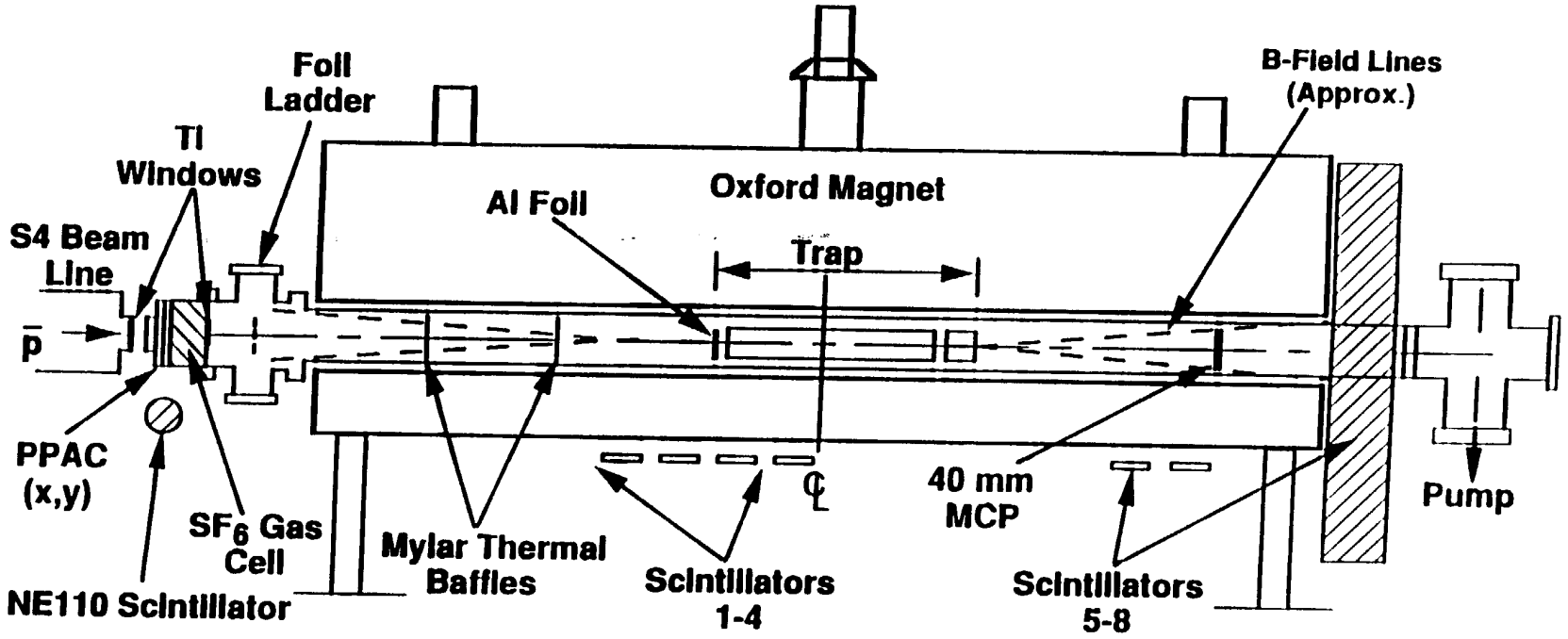
Foil
Ladder
Ti
Windows
S4 Beam
Line
$\bar{p}$
PPAC
(x,y)
NE110 Scintillator
SF_6 Gas
Cell
Mylar Thermal
Baffles
Al Foil
Oxford Magnet
Trap
B-Field Lines
(Approx.)
Scintillators
1-4
40 mm
MCP
Scintillators
5-8
Pump

Fig. 2

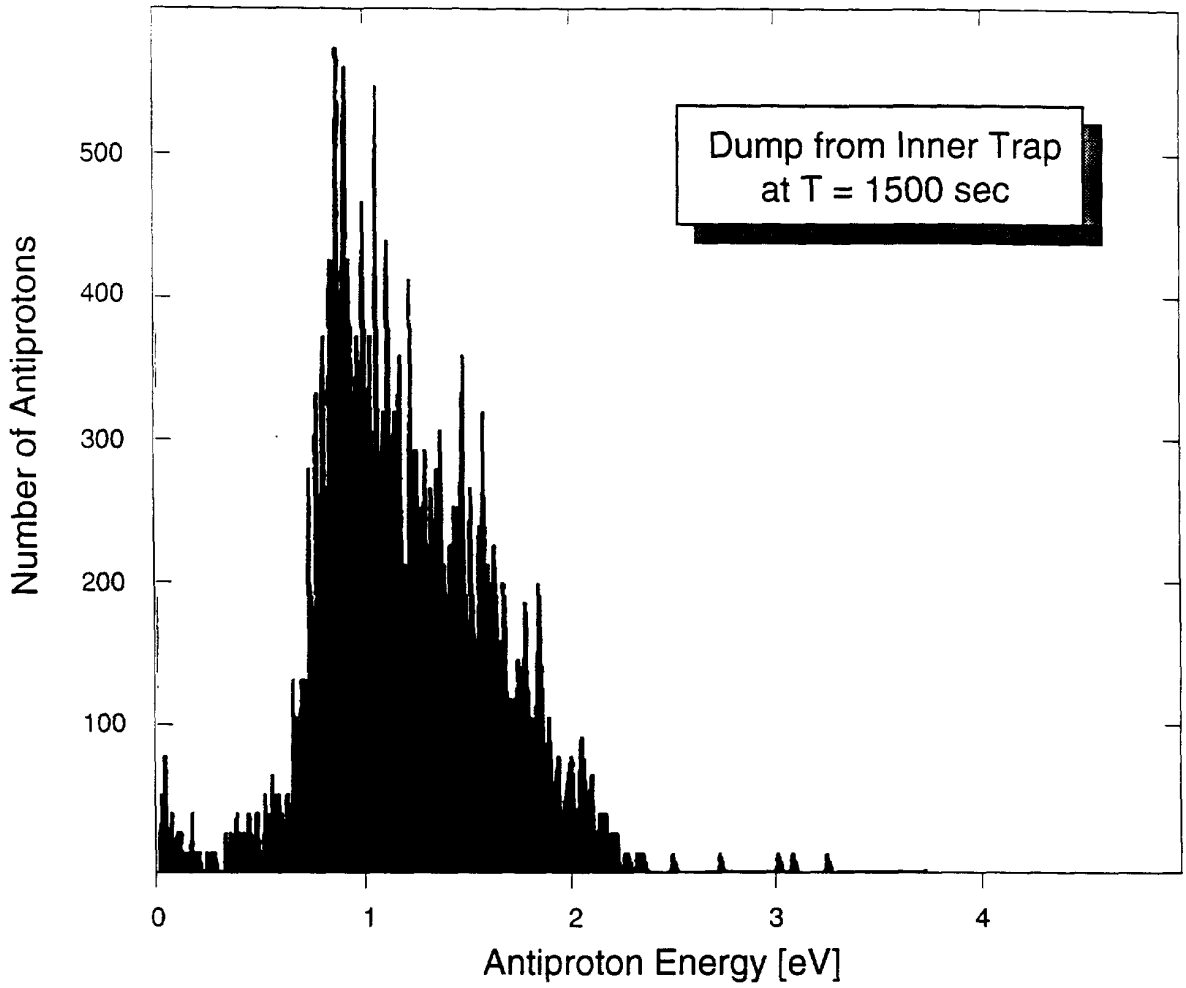
Dump from Inner Trap
at T = 1500 sec
Number of Antiprotons
500
400
300
200
100
0
1
2
3
4
Antiproton Energy [eV]

Fig. 3

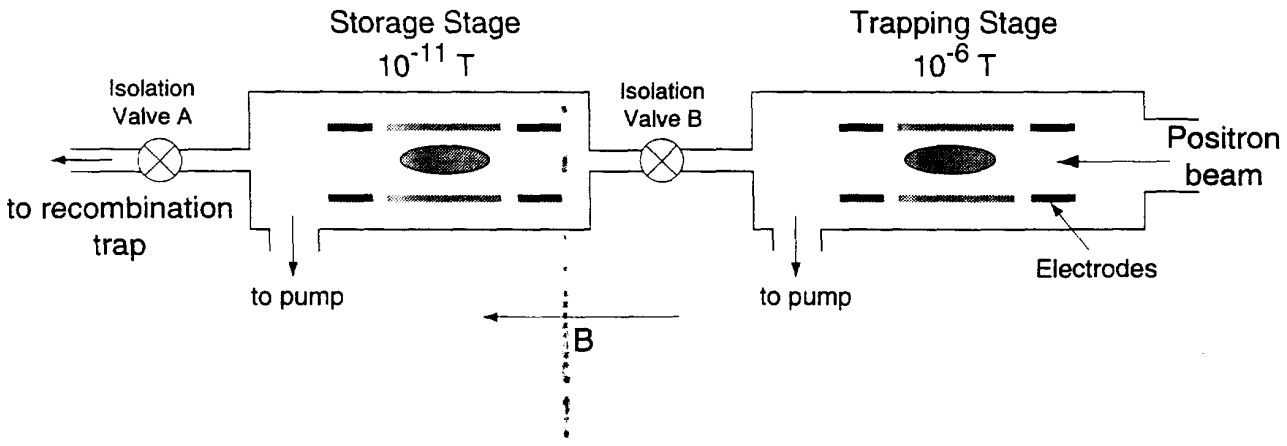
Storage Stage
10^{-11} T
Trapping Stage
10^{-6} T
Isolation
Valve A
Isolation
Valve B
Positron
beam
to recombination
trap
Electrodes
to pump
to pump
B

Fig. 4